Inorganic Chemistry
Article

Inorg. Chem. **2009**, *48*, 10819–10825 **10819**
DOI: 10.1021/ic901444c

Predicting the *Cis*−*Trans* Dichloro Configuration of Group 15−16 Chelated Ruthenium Olefin Metathesis Complexes: A DFT and Experimental Study

Charles E. Diesendruck,[†] Eyal Tzur,[†] Amos Ben-Asuly,[†,‡] Israel Goldberg,[⊥] Bernd F. Straub,[*,§] and N. Gabriel Lemcoff[*,†]

[†]*Chemistry Department, Ben-Gurion University of the Negev, Beer-Sheva 84105, Israel,* [‡]*Achva Academic College, Shikmim, Israel,* [§]*Organisch−Chemisches Institut, Universität Heidelberg, Heidelberg D-69120, Germany, and* [⊥]*School of Chemistry, Tel-Aviv University, Tel-Aviv 69978, Israel*

Received July 22, 2009

Gradient-corrected (BP86) and hybrid (M06-L) density functional calculations were used to study the relative stability of *cis* and *trans*-dichloro X-chelated benzylidene ruthenium complexes (X = O, S, Se, N, P). Calculations in the gas phase differed from experimental results, predicting the *trans*-dichloro configuration as being more stable in every case. The addition of Poisson−Boltzmann (PBF) continuum approximation (dichloromethane) corrected the disagreement and afforded energies consistent with experimental results. Novel N, Se, and P chelated ruthenium olefin metathesis complexes were synthesized to evaluate calculation predictions. These findings reinforce the importance of including solvent corrections in DFT calculations of ruthenium metathesis catalysts and predict that stronger σ donors as chelating atoms tend to electronically promote the unusual and less active *cis*-dichloro configuration.

Introduction

Olefin metathesis is one of the reactions that has most impacted organometallic and synthetic chemistry in the past decade.[1] Ruthenium catalysts (Figure 1) are especially interesting as a consequence of their higher stability and wider tolerance toward various functional groups.[1b] Since their first introduction by Grubbs,[2] these homogeneous catalysts have been enhanced both in their stability and reactivity by judicious alteration of their coordinative ligands. Perhaps the most significant improvement was achieved by the replacement of one of the phosphines by a stronger σ donor N-heterocyclic carbene (NHC),[3] which retarded initiation,[4] but stabilized the active conformation in the catalytic cycle.[5] An additional important modification was the exchange of the remaining phosphine ligand by a chelating oxygen,[6] which substantially improved catalyst stability, due to the chelating effect, while maintaining the same transition state.

On the basis of these pioneering results, many other modifications were introduced to influence catalyst activity[7] and stability.[8] While these changes generally did not affect the overall geometry of the complexes, occasionally, the unusual *cis*-dichloro structure was obtained as the most stable configuration.

After having been observed among the very first ruthenium alkylidenes,[9] the *cis*-dichloro structures were abandoned for many years, until Hofmann et al. prepared a chelating bidentate diphosphine ligand whereupon the two chlorides

*To whom correspondence should be addressed. (N.G.L.) Tel: +972-86461196. Fax: +972-86461740. E-mail: lemcoff@bgu.ac.il. (B.F.S.) Tel: +49-6221549239. Fax: +49-6221544205. E-mail: straub@oci.uni-heidelberg.de.

(1) (a) Hoveyda, A. H.; Zhugralin, A. R. *Nature* **2007**, *450*, 243–251. (b) Trnka, T. M.; Grubbs, R. H. *Acc. Chem. Res.* **2001**, *34*, 18–29. (c) Astruc, D. *New J. Chem.* **2005**, *29*, 42–56. (d) Fürstner, A. *Angew. Chem, Int. Ed.* **2000**, *39*, 3012–3043. (e) Schrock, R. R.; Czekelius, C. *Adv. Synth. Catal.* **2007**, *349*, 55–77. (f) Deshmukh, P. H.; Blechert, S. *Dalton Trans.* **2007**, 2479–2491.

(2) Nguyen, S. T.; Johnson, L. K.; Grubbs, R. H.; Ziler, J. W. *J. Am. Chem. Soc.* **1992**, *114*, 3974–3975.

(3) Scholl, M.; Ding, S.; Lee, C. W.; Grubb, R. H. *Org. Lett.* **1999**, *1*, 953–956.

(4) Sanford, M. S.; Love, J. A.; Grubbs, R. H. *J. Am. Chem. Soc.* **2001**, *123*, 6543–6554.

(5) (a) Straub, B. F. *Adv. Synth. Catal.* **2007**, *349*, 204–214. (b) Straub, B. F. *Angew. Chem., Int. Ed.* **2005**, *44*, 5974–5978. (c) Benitez, D.; Tkatchouk, E.; Goddard, W. A., III *Chem. Comm.* **2008**, 6194–6196.

(6) Garber, S. B.; Kingsbury, J. S.; Gray, B. L.; Hoveyda, A. H. *J. Am. Chem. Soc.* **2000**, *122*, 8168–8179.

(7) For a few examples of increased catalytic activity see: (a) Grela, K.; Harutyunyan, S.; Michrowska, A. *Angew. Chem., Int. Ed.* **2002**, *41*, 4038–4040. (b) Stewart, I. C.; Ung, T.; Pletnev, A. A.; Berlin, J. M.; Grubbs, R. H.; Schrodi, Y. *Org. Lett.* **2007**, *9*, 1589–1592. (c) Anderson, D. R.; Lavallo, V.; O'Leary, D. J.; Bertrand, G.; Grubbs, R. H. *Angew. Chem., Int. Ed.* **2007**, *46*, 7262–7265. (d) Castarlenas, R.; Vovard, C.; Fischmeister, C.; Dixneuf, P. H. *J. Am. Chem. Soc.* **2006**, *128*, 4079–4089. (e) Wakamatsu, H.; Blechert, S. *Angew. Chem., Int. Ed.* **2002**, *41*, 2403–2405.

(8) For a few examples of increased catalyst stability see: (a) Hong, S. H.; Grubbs, R. H. *J. Am. Chem. Soc.* **2006**, *128*, 3508–3509. (b) Foucault, H. M.; Bryce, D. L.; Fogg, D. E. *Inorg. Chem.* **2006**, *45*, 10293–10299. (c) Audic, N.; Clavier, H.; Mauduit, M.; Guillemin, J. -C. *J. Am. Chem. Soc.* **2003**, *125*, 9248–9249. (d) Vorfalt, T; Leuthäusser, S.; Plenio, H. *Angew. Chem., Int. Ed.* **2009**, *48*, 5191–5194.

(9) Nguyen, S. T.; Grubbs, R. H. *J. Am. Chem. Soc.* **1993**, *115*, 9858–9859.

Published on Web 10/20/2009

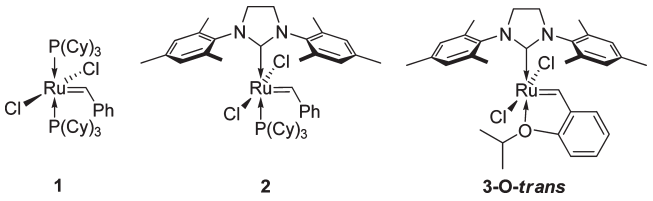

Figure 1. Ruthenium olefin metathesis initiators.

were forced to a *cis* arrangement.[10] Since, several *cis*-dichloro structures have been reported in the literature (Figure 2). In some cases the observed structures are obtained as a result of packing forces in crystals,[11] but other times they proved to be the stable configuration in solution.[12] Other anionic ligands in ruthenium alkylidenes may also be found in a *cis* configuration, for example, the use of catecholates by Fogg et al. as chelating anionic ligands.[13]

Density functional theory (DFT) calculations are a powerful tool for understanding and supporting mechanisms of organometallic reactions. They have been successfully used to investigate important aspects of olefin metathesis, such as initiation energies and mechanistic studies.[5,14] Notably, most of these studies disregarded the *cis* conformer, as it was shown to be less active than its *trans* isomer.[12d] Nonetheless, Goddard et al. studied a pyridine chelated system prepared by Grubbs,[12e] in which both *cis* and *trans* configurations could be observed in equilibrium in solution.[15] In this seminal work, it was shown that the addition of solvation energy in the DFT calculations was necessary to produce a reasonable agreement with the experimental results. However, all calculations were based on just a single complex. Based on our current interest in *cis*-dichloro latent chelated ruthenium catalysts, we decided to study additional complexes with different chelating atoms, where both *cis* and *trans* structures are observed. By relying on experimental data, and synthesizing further analogues when needed, correct parameters for accurate predictions may be obtained.

Results and Discussion

As a first step, different chelating atoms were compared to determine whether stronger σ donors are more stabilizing ligands in typical *trans*-dichloro complexes.

The 14-electron active species **8** is less stable than the 16-electron species. Thus, an olefin metathesis reaction between

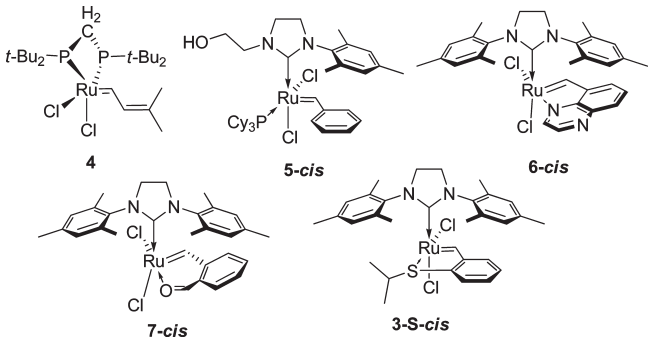

Figure 2. Some examples of known *cis*-dichloro ruthenium II alkylidene complexes.

8 and a chelating styrene (where the X atom may stabilize the metal center by a coordinative bond) is expected to afford **3-X-*trans*** (Scheme 1). Since the chelating atom in the product is *trans* to an extremely strong σ donor, this may generate a destabilizing *trans influence*.[16] Therefore, on one hand, strong σ donors may bind tighter to the metal, but on the other, a more significant *trans influence* may destabilize the complex.

The optimized structures were obtained with BP86/LACVP* theory level in the gas-phase, followed by single-point energy calculations using BP86/LACV3P**++ theory level. The results are summarized in Table 1.

The order of stability was X = O < *N* < S $\approx$ Se < P, signifying that the energy gained by better σ donors is more significant than the destabilizing *trans influence*; i.e., better σ donors bind stronger and stabilize the metal center more efficiently. Interestingly, calculations show a clear increase in the Cl−Ru−Cl angle as the ligand binds stronger. This angle decreases with weaker ligands to compensate for the stronger σ donation of the carbene.[5a]

Once the energetics of the metathesis reaction were studied, the difference between the *cis* and *trans* structures could be addressed. Accordingly, the complexes **3-X** were calculated in both configurations (Figure 3) using BP86/LACV3P**++// BP86/LACVP* (Figure 4) and M06-L/LACV3P**++// LACVP* (see the Supporting Information).

Starting geometries for *cis* compounds were obtained from the X−ray diffraction structure of sulfur complex **3-S-*cis***,[12a] while the **3-O-*trans*** structure was used as a starting point for all trans complexes.[6]

In all cases, the addition of solvation parameters stabilized the more polar *cis* structures by a similar value. This stabilization is more meaningful for phosphorus, sulfur, and selenium, where the *trans*-dichloro configuration is predicted to appear in the gas phase, but the *cis*-dichloro isomer is calculated to be the sole species in solution. As seen in Figure 4, calculations strongly suggest that weaker σ donor chelates, such as oxygen, should be more stable in the *trans*-dichloro configuration. On the other hand, when a strong *trans influence* is present, the Ru−X bond is severely weakened, disfavoring the *trans*-dichloro arrangement. As this effect is immaterial in the *cis*-dichloro configuration, the chelating ligand may sit closer to the metal center and stronger donors may form a stronger bond. Indeed, the

(10) Hansen, S. M.; Rominger, F.; Metz, M.; Hofmann, P. *Chem.—Eur. J.* **1995**, *5*, 557–566.

(11) (a) Barbasiewicz, M.; Bieniek, M.; Michrowska, A.; Szadkowska, A.; Makal, A.; Wozniak, K.; Grela, K. *Adv. Synth. Catal.* **2007**, *349*, 193–203. (b) Pruhs, S.; Lehmann, C. W.; Fürstner, A. *Organometallics* **2004**, *23*, 280–287.

(12) (a) Ben-Asuly, A.; Tzur, E.; Diesendruck, C. E.; Sigalov, M.; Goldberg, I.; Lemcoff, N. G. *Organometallics* **2008**, *27*, 811–813. (b) Kost, T.; Sigalov, M.; Goldberg, I.; Ben-Asuly, A.; Lemcoff, N. G. *J. Organomet. Chem.* **2008**, *693*, 2200–2203. (c) Diesendruck, C. E.; Vidavsky, Y.; Ben-Asuly, A.; Lemcoff, N. G. *J. Polym. Sci., Part A: Polym. Chem.* **2009**, *47*, 4209–4213. (d) Barbasiewicz, M.; Szadkowska, A.; Bujok, R.; Grela, K. *Organometallics* **2006**, *25*, 3599–3604. (e) Ung, T.; Hejl, A.; Grubbs, R. H.; Schrodi, Y. *Organometallics* **2004**, *23*, 5399–5401. (f) Slugovc, C.; Perner, B.; Stelzer, F.; Mereiter, K. *Organometallics* **2004**, *23*, 3622–3626.

(13) (a) Monfette, S.; Fogg, D. E. *Organometallics* **2006**, *25*, 1940–1944. (b) Monfette, S.; Camm, K. D.; Gorelsky, S. I.; Fogg, D. E. *Organometallics* **2009**, *28*, 944–946.

(14) (a) Occhipinti, G.; Bjørsvik, H. -R.; Jensen, V. R. *J. Am. Chem. Soc.* **2006**, *128*, 6952–6964. (b) Correa, A.; Cavallo, L. *J. Am. Chem. Soc.* **2006**, *128*, 13352–13353.

(15) Benitez, D.; Goddard, W. A., III *J. Am. Chem. Soc.* **2005**, *127*, 12218–12219.

(16) (a) Toledo, J. C.; Neto, B. S. L.; Franco, D. W. *Coord. Chem. Rev.* **2005**, *249*, 419–431. (b) Appleton, T. G.; Clark, H. C.; Manzer, L. E. *Coord. Chem. Rev.* **1973**, *10*, 335–422.

Scheme 1. Metathesis Reaction with X-Chelating Styrene

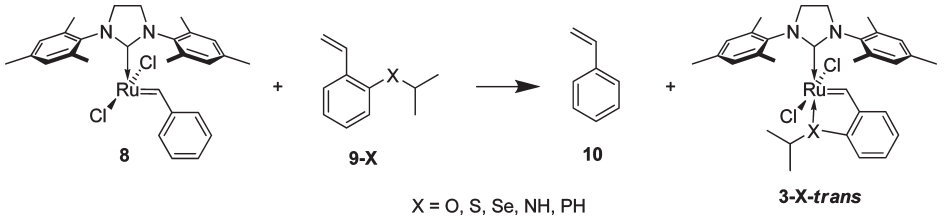

Table 1. Stabilization Energies in the Formation of **3-X-*trans***

chelating atom	$\triangle E$ gas phase (kJ mol^{-1})[a]	Cl−Ru−Cl angle (°)
oxygen	31.5	155.8
nitrogen	48.1	159.6
sulfur	58.4	162.4
selenium	59.0	161.6
phosphorus	93.5	163.3

[a] $\triangle E = E$(**9-X**) + E(**8**) − E(**3-X-*trans***) − E(10).

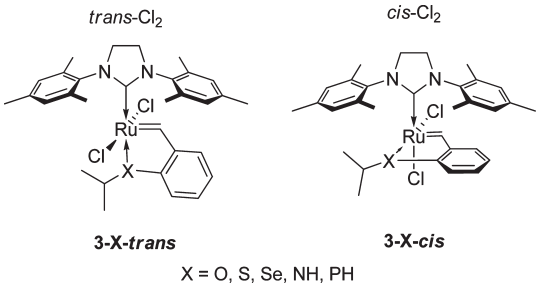

Figure 3. Complexes analyzed in our DFT calculations.

Ru−X bond distances are shorter for second row and lower atoms in the *cis* configuration (Table 2).

The BP86 calculations were in line with known and herein presented (*vide infra*) solid state data. For example, for the complex **3-O-*trans***, the calculations predicted a distance of 2.31 Å compared to 2.26 Å observed in the crystal structure. Recently, several scientific publications demonstrated how the M06-L functional,[17] which is a hybrid meta-GGA exchange-correlation functional developed to include attractive medium-range (van der Waals or London dispersion) interactions presented improved results in olefin metathesis ruthenium complexes.[18] Structural optimizations using M06-L resulted in very similar structures as compared to BP86. However, M06-L calculations showed a tendency to prefer the *cis*-dichloro isomers, although the general overall trends were preserved.

Cis isomers of **3-O-*trans*** or other 5-membered ring sp^3 O-chelated complexes have not been observed experimentally in solution, in accordance with calculations that predict that oxygen and nitrogen chelates should be more stable as the *trans* isomers. However, while several sp^2 nitrogen chelated complexes have been prepared,[12c,d,19] we are unaware of sp^3 nitrogen chelated complexes in the literature. In addition, chelated selenium and phosphorus benzylidenes were also unknown. Therefore, we decided to prepare simple sp^3 nitrogen, selenium, and phosphorus chelated complexes to evaluate our theoretical predictions (Schemes 2−4).

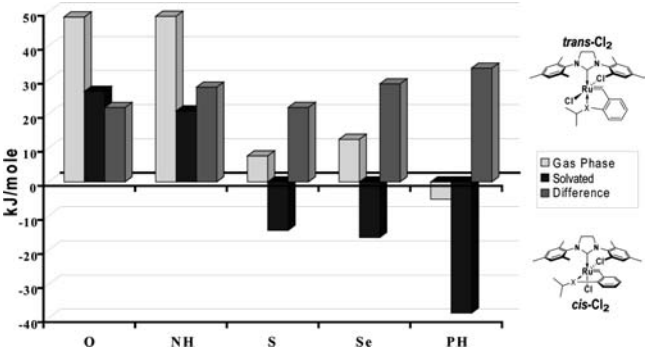

Figure 4. Difference ($\triangle E$) in energy (kJ mol^{-1}) between *cis*-dichloro and *trans*-dichloro configurations.

Starting from commercially available 2-fluorobenzaldehyde, a diethyl amino group was introduced by a nucleophilic aromatic substitution. A concurrent Wittig reaction converted the carbonyl into the appropriate styrene derivative, and metathesis in the presence of (NHC)(Py)$_2$(Cl)$_2$Ru=CHPh produced the desired complex **14**. Suitable crystals of **14** confirmed the *trans*-dichloro geometry (Figure 5). NMR analyses showed a symmetric structure supporting the same *trans* arrangement also in solution (see the Supporting Information).

The synthesis of the Se-chelated complex was somewhat more involved than the N-, S-, and O-chelated complexes. Following a known procedure,[20] a selenocyanate group was inserted into starting material **15** by reacting its diazo derivative with potassium selenocyanate. Reduction of the ester group followed by exposure to air provided dimer **17**, which could be readily oxidized to the di-aldehyde with pyridinium chlorochromate. The diselenide bond was broken with isopropyl iodide and a Wittig reaction afforded styrene derivative **20**, which was then reacted by olefin metathesis with **2** in the presence of CuCl to obtain the desired complex. Only the *cis*-dichloro product was observed in solution (NMR). X-ray structure analysis confirmed the observed configuration (Figure 6).

A complex comparable to **3-P** could be prepared starting from commercially available **21**. This was readily achieved by a simple Wittig reaction followed by metathesis to afford the desired complex **23**.

Also in this case, the -ray structure obtained was characterized as the *cis* isomer (Figure 7).

(17) Zhao, Y.; Truhlar, D. G. *Acc. Chem. Res.* **2008**, *41*, 157–167.

(18) (a) Benitez, D.; Tkatchouk, E.; Goddard, W. A., III *Organometallics* **2009**, *28*, 2643–2645. (b) Zhao, Y.; Truhlar, D. G. *Org. Lett.* **2007**, *9*, 1967–1970. (c) Torker, S.; Merki, D.; Chen, P. *J. Am. Chem. Soc.* **2008**, *130*, 4808–4814. (d) Fedorov, A.; Moret, M.-E.; Chen, P. *J. Am. Chem. Soc.* **2008**, *130*, 8880–8881.

(19) (a) van der Schaaf, P. A.; Kolly, R.; Kirner, H. J.; Rime, F.; Muhlebach, A.; Hafner, A. *J. Organomet. Chem.* **2000**, *606*, 65–74. (b) Slugovc, C.; Burtscher, D.; Stelzer, F.; Mereiter, K. *Organometallics* **2005**, *24*, 2255–2258. (c) Barbasiewicz, M.; Szadkowska, A.; Bujok, R.; Grela, K. *Organometallics* **2006**, *25*, 3599–3604. (d) Hejl, A.; Day, M. W.; Grubbs, R. H. *Organometallics* **2006**, *25*, 6149–6154.

(20) Iwaoka, M.; Tomoda, S. *Phosphorus, Sulfur Silicon Relat. Elem.* **1992**, *67*, 125–130.

Table 2. Calculated and Experimental Ru−X Bond Length for Chelated Complexes **3-X**

chelating atom X	*trans* bond length (Å) (calc. BP86)	*cis* bond length (Å) (calc. BP86)	*trans* bond length (Å) (calc. M06-L)	*cis* bond length (Å) (calc. M06-L)	experimental Ru−X bond length (Å)
oxygen	2.31	2.41	2.36	2.39	2.26 (*trans*)
nitrogen[a]	2.32	2.31	2.35	2.36	2.34 (*trans*)
sulfur	2.54	2.42	2.60	2.43	2.35 (*cis*)
selenium	2.68	2.57	2.66	2.60	2.46 (*cis*)
phosphorus[b]	2.38	2.32	2.36	2.30	2.31 (*cis*)

[a] Calculated structure is **3-NH**, X−ray structure is **14**. [b] Calculated structure is **3-PH**, X−ray structure is **23**.

Scheme 2. Preparation of N−Chelated Olefin Metathesis Complex

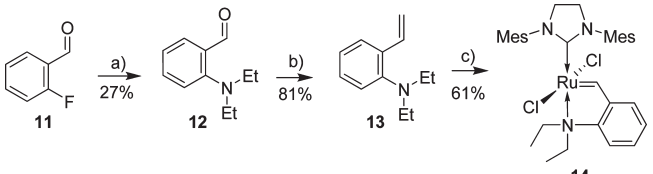

a) K_2CO_3, Et_2NH, DMF, b) CH_3PPh_3I, KOtBu, Et_2O, c) $(NHC)(Py)_2(Cl)_2Ru=CHPh$, CH_2Cl_2.

In all cases NMR and solid state analyses afforded the same configurations for the complexes studied. Figure 8 displays the four methylene hydrogens in the symmetric *trans* **14** as a singlet signal, while **23** and **3-Se-*cis*** present the typical complex imidazoline-2-ylidene splitting patterns observed for *cis*-dichloro structures.

As shown in Table 2, for sulfur complex **3-S-*cis*** the Ru−X distance predictions were satisfactory, i.e., 2.42 Å in calculations compared to 2.35 Å in the X-ray structure.[12a] The X-ray structures of **3-Se-*cis*** and 23 showed Ru−X bond lengths of 2.457 and 2.31 Å (average of 2 different molecules in the unit cell) compared to 2.57 and 2.32 Å obtained in the calculations. Thus, for all heteroatoms studied, the Ru−X bond lengths could be fairly well reproduced (within 0.1 Å) using both BP86 and M06-L.

The N-chelated structures also presented a very close similarity between calculated and experimental X-ray data. The Ru−N bond length observed in the crystal structure was 2.336 Å, while the calculations provided a bond length of 2.32 Å. The availability of other nitrogen types and their mixed configurations (both *cis* and *trans*-dichloro structures have been experimentally observed) presented the opportunity to analyze these additional compounds and evaluate the computational predictions for another known *cis*-dichloro molecule (Figure 9). Complex **3-NH-*trans*** has an sp^3 nitrogen (similar to **14**), while the nitrogen in **24** has an sp^2 hybridization and **25** an aromatic sp^2 N.

BP86/LACV3P**++ gas-phase calculations predicted a *trans* arrangement for the three N-chelated complexes, as observed experimentally for **14** and an analogue of **24**.[21] However, Grela's quinoline complex **25**[12d] was shown experimentally to retain a *cis* configuration in solution. Thus, BP86 gas-phase calculations could not correctly predict the configuration of the complex. Once again, the addition of solvation effects (Table 3) drastically changed the $\triangle E$, affording results consistent with experimental findings in all the N-chelated complexes. The solvated *cis*-dichloro complex **24** is predicted to be more stable with M06-L model calculations, whereas the *trans*-dichloro structure has been obtained

Table 3. Difference in *cis*−*trans* Energies for N-Chelated Ruthenium Complexes with BP86 (M06-L) Functionals

Complex	$\triangle E$ (kJ mol^{-1}) in gas phase[a]	$\triangle E$ (kJ mol^{-1}) solvated[a]	experimental observation
3-NH	48.7 (40.0)	20.8 (9.0)	*trans*[b]
24	31.6 (17.3)	7.4 (−13.8)	*trans*[c]
25	12.2 (−6.2)	−13.5 (−35.7)	*cis*/*trans* = *78*/*22*

[a] $\triangle E$ = *E*(**cis**) − *E*(**trans**). [b] For related complex **14**. [c] See reference 21.

experimentally.[21] The differences of zero point energies for *cis*- and *trans*-dichloro complexes are negligible, while the corrections for Gibbs Free energies consistently stabilize *trans*-dichloro complexes by an additional 4−14 kJ mol^{-1}. This leads to a reasonable agreement for the BP86 calculations in the case of complex **25**, where a *cis*/*trans* equilibrium is observed in solution (Table 3).[12d] The M06-L functionals feature either worse accuracy or less error cancellation. In line with this finding, M06-L functionals have been reported to predict significantly higher Ru−P bond dissociation energies (151.4−174.5 kJ mol^{-1} and 159.8−189.1 kJ mol^{-1})[18b] for Grubbs I and Grubbs II catalysts than the dissociative PCy_3 ligand barriers derived from NMR measurements (83.2 ± 0.3 and 96.2 ± 1.7 kJ mol^{-1}).[4] Thus, M06-L should still be used with caution in ruthenium carbene chemistry.

For sulfur chelates, the *trans* isomer may be observed (and isolated) as a kinetic product, but it is completely converted into the *cis* isomer in solution and even in the solid phase.[12a] Notably, even the additional steric energy obtained by the exchange of the isopropyl substituent in **3-S** for a *t*-butyl group[12b] did not promote a configuration change. Thus, both sulfur and selenium compounds that are calculated in the gas phase to be more stable in the *trans*-dichloro configuration are correctly predicted to be *cis* when solvent effects are added.

The strong propensity of the phosphorus compound to remain in the *cis*-dichloro configuration may seem at first sight incongruous with the observation that non-chelated catalyst **2** is more stable as the *trans*-dichloro isomer. Two effects seem to be affecting the configuration in this case. First of all, the three bulky cyclohexyl groups on P could create significant steric repulsions if the phosphine would be *cis* to the NHC ligand. Additionally, π-stacking between the benzylidene ring and the mesityl ring,[11b,12a,12f] would be disrupted if the PCy_3 ligand occupied the *cis* position. However, smaller phosphine ligands could lessen steric hindrance and promote a change in the ligand geometry. Complexes related to **2** with smaller phosphines, such as trimethylphosphine[22] and triisopropylphosphine[23] are known. Even though the literature describes

(21) Slugovc, C.; Burtscher, D.; Stelzer, F.; Mereiter, K. *Organometallics* **2005**, *24*, 2255–2258.

(22) Bolton, S. L.; Williams, J. E.; Sponsler, M. B. *Organometallics* **2007**, *26*, 2485–2487.

(23) Eide, E. F. V. D.; Romero, P. E.; Piers, W. E. *J. Am. Chem. Soc.* **2008**, *130*, 4485–4491.

Scheme 3. Synthesis of Selenium Chelated Olefin Metathesis Complex

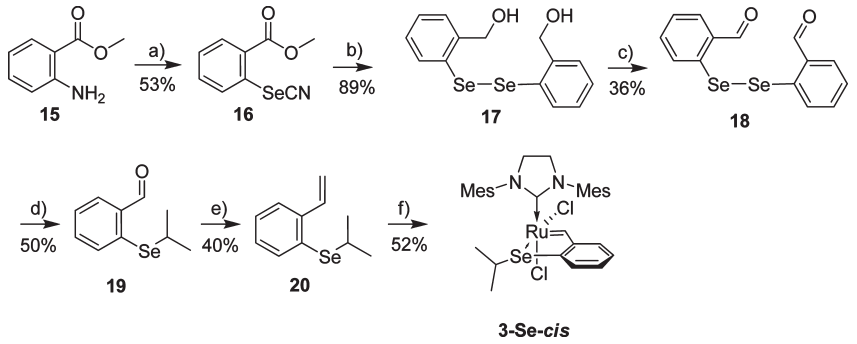

a) 1) $NaNO_2$, HCl, 2) KSeCN, H_2O; b) 1) $LiAlH_4$, Et_2O, 2) O_2; c) PCC, CH_2Cl_2; d) KOH, DMSO, $(CH_3)_2CHI$; e) CH_3PPh_3I, KOtBu, Et_2O; f) **2**, CuCl, CH_2Cl_2.

Scheme 4. Synthesis of Phosphorous Chelated Olefin Metathesis Complex

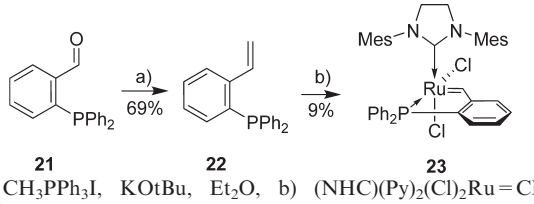

a) CH_3PPh_3I, KOtBu, Et_2O, b) $(NHC)(Py)_2(Cl)_2Ru=CHPh$, CH_2Cl_2.

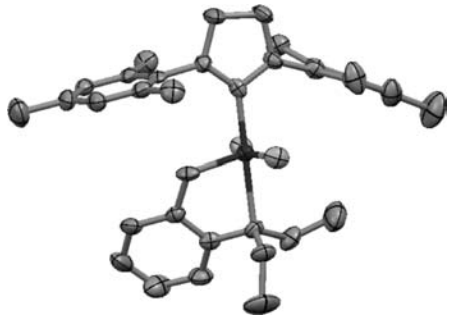

Figure 5. X-ray structure of complex **14**.

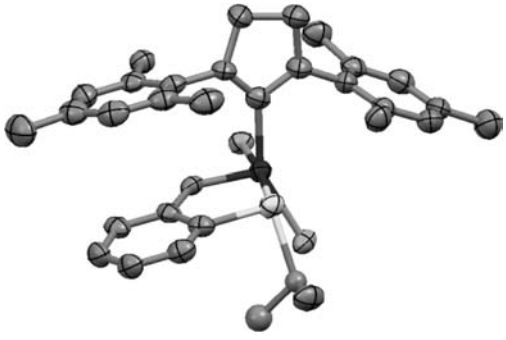

Figure 6. ORTEP of selenium-chelated olefin metathesis complex **3-Se-*cis*** (**see Experimental Section**).

these complexes in the *trans*-dichloro configuration, in both cases the mesityl methyl group signals in the ^1H-NMR spectrum appear as six separate peaks and the imidazolidine methylene hydrogens are described as multiplets, indicating an asymmetric configuration corresponding to a *cis*-dichloro geometry. Unfortunately, no X-ray structures for these P-coordinated complexes were reported in these studies. In

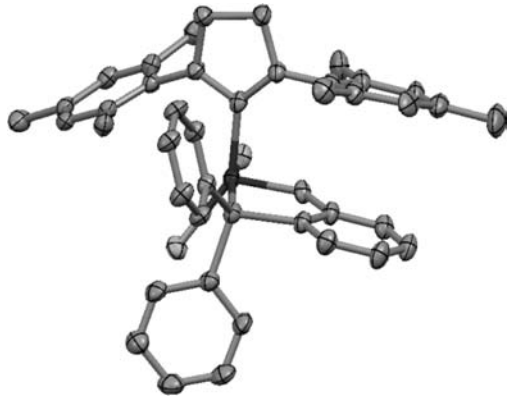

Figure 7. Phosphorus-chelated olefin metathesis complex **23**.

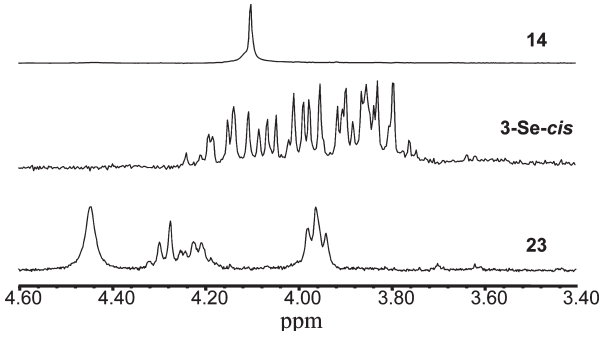

Figure 8. Methylene region in complexes **14**, **3-Se-*cis*, and 23**.

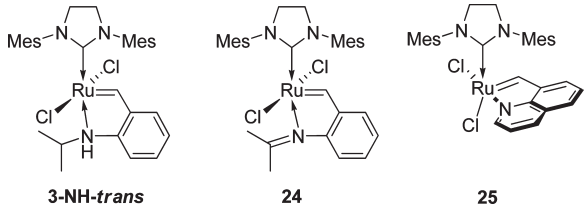

Figure 9. N-Chelated ruthenium olefin metathesis complexes calculated.

the case of novel chelated complex **23** with relatively bulky phenyl groups, the steric hindrance is beautifully alleviated by the insertion of one of the phenyl substituents on the phosphorus between the NHC mesityl methyl groups (Figure 7). Naturally, π-stacking with the benzylidene in the chelated complexes may exist only in the *cis* configuration.

Conclusions

DFT calculations both in gas phase and with solvation effects were carried out for a series of nitrogen group and chalcogen chelated ruthenium benzylidene complexes, both in *cis*-dichloro and *trans*-dichloro configurations. Also, novel nitrogen, selenium, and phosphorus chelated ruthenium complexes were prepared and structurally analyzed to provide additional experimental support. Solvation stabilized the higher dipole moment of *cis*-dichloro structures compared to the isomeric *trans*-dichloro complex, in which the two local Ru−Cl dipole moments neutralize each other and afforded results more in line with experimental findings. We observed that a stronger σ donation character of the chelating atom strengthened the bond to the ruthenium and increased the tendency to obtain a stable *cis*-dichloro configuration. π acids (such as phosphines) electronically prefer to be *trans* to a π donor (such as Cl); while weak σ and π donors (for example ethers) favor a *trans* position to a strong σ donor and π acceptor (NHC); but sterically demanding NHCs and ligands with bulky substituents still tend to assume a *trans* configuration (like in **2** − the NHC is observed *trans* to PCy_3). The p(Cl) orbitals also play a role in the stability of the different configurations. While we showed here how the Cl−Ru−Cl angles change according to the different acceptors, a more profound study is underway to analyze how the anionic ligands may ultimately also alter the final configuration.

Being able to predict the configuration of chelated ruthenium complexes is of importance in the design of new catalysts. For example, the known reduction in reactivity of the *cis*-dichloro forms in ruthenium alkylidenes may be implemented in the preparation of latent olefin metathesis catalysts.[24] The results presented herein clearly show how DFT calculations of chelated ruthenium benzylidenes may show guidance to direct future experiments.

Experimental Section

General. All reagents were of reagent grade quality, purchased commercially from Sigma, Aldrich, Fluka, or ABCR and used without further purification. All solvents were dried and distilled prior to use. Purification by column chromatography was performed on Davisil chromatographic silica media (40−60 μm). TLC analyses were performed using Merck pre−coated silica gel (0.2 mm) aluminum [backed] sheets. NMR spectra were recorded on Bruker DPX_{200} or DMX_{500} instruments; chemical shifts, given in ppm, are relative to Me_4Si as the internal standard, or using the residual solvent peak. MS data were obtained using an Agilent 6850 GC equipped with an Agilent 5973 MSD working under standard conditions and an Agilent HP5-MS column, a Bruker Daltonics Ion Trap MS Esquire 3000 Plus equipped with APCI (atmospheric pressure chemical ionization) or on a mass spectrometer with an ESI source (Thermo Fisher Scientific), where spectra were collected in the positive ion mode and analyzed by Xcalibur software (Thermo Fisher Scientific). $(NHC)(Py)_2(Cl)_2Ru=CHPh$ was prepared according to a known procedure.[25]

Calculation Methods. The quantum-chemical calculations were carried out using DFT.[26] The calculations employed a combination of the Becke exchange[27] and Perdew correlation[28] functionals (BP86), or M06-L[17] which were shown[13b,18,29] to afford good results with ruthenium olefin metathesis complexes. The 28 inner core electrons of the ruthenium atom were described with the Hay and Wadt small-core-valence relativistic effective-core-potential leaving the outer electrons to be treated explicitly.[30] All electrons for other atoms were considered with the 6-31G* or 6-31G**++ basis set.[31]

The structures were optimized without constraints and minima were found using LACVP* level of theory with Jaguar. The optimized stationary points were characterized as minima by analytic computation of the harmonic force constants. The energies were then determined using LACV3P**++ for higher level calculations.

Solvation energies were calculated using the Poisson−Boltzmann (PBF) continuum approximation, with dichloromethane as a solvent, as offered in Jaguar 7.0.[32]

2-(Diethylamino)benzaldehyde (12). 2-Fluorobenzaldehyde (2.00 gr, 16.1 mmol), K_2CO_3 (3.6 gr, 26.1 mmol), and diethylamine (2.68 gr, 36.6 mmol) were added to 10 mL of DMF. The mixture was stirred at 65 °C for 3 days, poured into 100 mL of saturated $NaHCO_3$, and extracted with CH_2Cl_2. The organic phase was dried with sodium sulfate and evaporated, and the residue was purified by column chromatography (hexane 200:3 ether), affording a yellow oil after evaporation (0.765 gr, 27%). ^{1}H-NMR and ^{13}C-NMR (200 and 50 MHz, $CDCl_3$) in accordance to literature.[33] GC−MS: m/z M^+ Calcd 177.12, found 177.10.

N,N-Diethyl-2-vinylbenzenamine (13). Methyl triphenylphosphonium iodide (1.57 gr, 3.88 mmol) was dissolved in 25 mL of ether in a 50-mL round-bottom flask at 0 °C under dry nitrogen. Potassium *tert*-butoxide (0.47 gr, 4.16 mmol) was added in one portion to the mixture and then it was stirred for 10 min at room temperature, followed by addition of **12** (0.49 gr, 2.77 mmol) stirring for an additional 2 h at room temperature. The mixture was added to 200 mL of saturated sodium bicarbonate solution, and extracted with 3 × 80 mL portions of ether. The extracts were dried with magnesium sulfate and evaporated. The crude product was further purified by chromatography on silica gel using a mixture of petroleum ether and ether (10:1) as eluent to afford a colorless oil after evaporation (391 mg, 81%). ^{1}H-NMR (500 MHz, $CDCl_3$): 7.53 (dd, 1H), 7.22 (dt, 1H), 7.17 (dd, 1H), 7.07−7.02 (m, 2H), 5.66 (dd, 1H), 5.21 (dd, 1H), 3.05 (q, 4H), 1.00 (t, 6H). ^{13}C-NMR (125 MHz, $CDCl_3$): 149.1, 134.8, 134.4, 127.8, 126.3, 122.8, 121.8, 112.7, 47.3, 12.2. GC−MS: m/z M^+ Calcd 175.14, found 175.10.

Complex 14. $(NHC)(Py)_2(Cl)_2Ru=CHPh$ (116 mg, 0.16 mmol), **13** (30.8 mg, 0.18 mmol) and CH_2Cl_2 (6 mL) were added to a pressure flask. The flask was closed and the solution was stirred at 40 °C for 5 h. The solvent was evaporated and the product was purified by column chromatography using hexane/acetone (7:3) as eluent. An office green solid was obtained (61 mg, 61%). ^{1}H-NMR (500 MHz, CD_2Cl_2): 16.7 (s, 1H), 7.47 (dt, 1H), 7.10 (br s, 2H), 7.07−7.04 (m, 2H), 7.00 (br s, 2H), 6.81 (dd, 1H), 4.09 (s, 4H), 3.16 (q, 2H), 2.54 (br s, 6H), 2.45 (br s, 2H), 2.32 (br s, 12H), 0.48 (t, 6H). ^{13}C-NMR (125 MHz, CD_2Cl_2): 302.1, 211.5, 157.0, 150.4, 139.8, 138.7, 137.9, 137.7, 134.3,

(24) Ben-Asuly, A.; Aharoni, A.; Diesendruck, C. E.; Vidavsky, Y.; Goldberg, I.; Straub, B. F.; Lemcoff, N. G. *Organometallics* **2009**, *28*, 4652–4655.
(25) Sanford, M. S.; Love, J. A.; Grubbs, R. H. *Organometallics* **2001**, *20*, 5314–5318.
(26) (a) Parr, R. G.; Yang, W. *Density Functional Theory of Atom and Molecules*; Oxford University Press: New York, 1989. (b) Koch, W.; Holthausen, M. C. *A Chemist's Guide to Density Functional Theory*; Wiley−VCH: Weinheim, 2000.
(27) Becke, A. D. *Phys. Rev. A* **1988**, *38*, 3098–3100.
(28) Perdew, J. P. *Phys. Rev. B* **1986**, *33*, 8822–8824.
(29) Vyboishchikov, S. F.; Buhl, M.; Thiel, W. *Chem.—Eur. J.* **2002**, *8*, 3962–3975.
(30) Hay, P. J.; Wadt, W. R. *J. Chem. Phys.* **1985**, *82*, 299–310.
(31) Hariharan, P. C.; Pople, J. A. *Chem. Phys. Lett.* **1972**, *16*, 217–219.
(32) *Jaguar 7.0*; Schrodinger, LLC: Portland, OR, 2007. CH_2Cl_2 was used as a model solvent − ε = 8.93, solvent radius = 2.33 Å.
(33) Nate, H.; Sekine, Y.; Honma, Y.; Nakai, H.; Wada, H.; Takeda, M.; Yabana, H.; Nagao, T. *Chem. Pharm. Bull.* **1987**, *35*, 1953–1968.

129.3, 128.8, 127.3, 127.0, 123.4, 117.8, 51.7, 51.0, 49.8, 21.0, 20.8, 20.4, 18.1, 10.0. FAB−MS: m/z $[M]^+$ Calcd 639.17, found 639.3. Single crystals were successfully grown by slow diffusion of pentane in a solution of **14** in CH_2Cl_2 at −18 °C.

$C_{32}H_{41}Cl_2N_3Ru$, M = 639.65, monoclinic, space group $C2/c$, a = 39.258(18), b = 11.887(5), c = 14.358(6) Å, β = 106.845(9)°, V = 6413(5) Å^3, Z = 8, T = 200(2) K, ρ_{calcd} = 1.325 g cm^{-3}, μ(Mo Kα) = 0.68 mm^{-1}, 14787 reflections measured ($2\theta_{max}$ = 51.4°), 5693 unique (R_{int} = 0.13), final R = 0.065 (wR = 0.139) for 3104 reflections with $I > 2\sigma(I)$ and R = 0.144 (wR = 0.179) for all data, $\Delta|\rho_{max}|$ = 1.31 e/Å^3.

Methyl 2-selenocyanatobenzoate (16) and **bis[2-(hydroxymethyl)phenyl]diselenide (17)** were prepared according to known procedures.[20]

Bis(2-formylphenyl) Diselenide (18). 17 (1.00 gr, 2.69 mmol) was dissolved in 100 mL of CH_2Cl_2 in a round-bottomed flask. The solution was cooled with ice, followed by addition of pyridinium chlorochromate (1.45 gr, 6.725 mmol) in small portions. The mixture was further stirred for 1 h at 0 °C, and then filtered and evaporated. Purification by column chromatography using petrol ether and ethyl acetate (6:1) as eluent afforded **18** (362 mg, 36%). ^{1}H-NMR and ^{13}C-NMR (200 and 50 MHz, $CDCl_3$) in accordance to literature.[34] GC−MS: m/z M^+ Calcd 369.90, found 369.90.

2-(Isopropylselanyl)benzaldehyde (19). To a flame-dried round-bottomed flask, KOH (400 mg, 7.1 mmol), DMSO (15 mL), **18** (148 mg, 0.4 mmol), and *iso*-propyliodide (510 μL, 5.1 mmol) were added, and the mixture was stirred for 4 h. Water (20 mL) was then added and the mixture was extracted with CH_2Cl_2 (3 × 50 mL). The organic phase was dried over $MgSO_4$ and evaporated. The pure product **21** was obtained after purification by column chromatography using petrol ether and ethyl acetate (10:1) as eluent (90 mg, 50%). ^{1}H-NMR (200 MHz, $CDCl_3$): 10.38 (s, 1H), 7.87 (dd, 1H), 7.64 (dd, 1H), 7.53−7.35 (m, 2H), 3.52 (hept, 1H), 1.46 (d, 6H). ^{13}C-NMR (50 MHz, $CDCl_3$): 193.4, 136.3, 136.0, 133.8, 133.5, 132.1, 126.7, 32.9, 23.7. GC−MS: m/z M^+ Calcd 228.01, found 228.00.

Isopropyl(2-vinylphenyl)selane (20). Methyl triphenylphosphonium iodide (222 mg, 0.55 mmol) was dissolved in 8 mL of ether in a 50-mL round-bottomed flask at 0 °C under dry nitrogen. To the mixture was added in one portion potassium *tert*-butoxide (68 mg, 0.60 mmol) and it was stirred for 10 min at room temperature. **19** (90 mg, 0.396 mmol) was added in one portion at 0 °C and the reaction mixture was stirred for additional 4 h at room temperature. The mixture was poured into 25 mL of saturated sodium bicarbonate solution, and extracted with 3 × 20 mL portions of ether. The extracts were dried with magnesium sulfate and evaporated. The light yellow oil of the crude product was further purified by chromatography on silica gel using petroleum ether as eluent to afford a colorless oil (36 mg, 40%). ^{1}H-NMR (200 MHz, $CDCl_3$): 7.59 (d, 1H), 7.58 (dd, 1H), 7.39−7.13 (m, 3H), 5.65 (dd, 1H), 5.29 (dd, 1H), 3.41 (hept, 1H), 1.38 (d, 6H). ^{13}C-NMR (50 MHz, $CDCl_3$): 141.0, 137.3, 136.1, 130.1, 128.0, 127.9, 125.8, 115.4, 34.1, 24.1. GC−MS: m/z M^+ Calcd 226.03, found 226.00.

Complex 3-Se-*cis*. CuCl (20 mg, 0.20 mmol) and **2** (109 mg, 0.128 mmol) were added to a pressured flask. CH_2Cl_2 (4 mL) was added and the mixture was stirred for 5 min. **20** (33 mg, 0.146 mmol) in CH_2Cl_2 (2 mL) was added. The flask was closed and the mixture was stirred at 40 °C for 4 h. The solvent was evaporated and the product was purified by chromatography on silica gel using petroleum ether and acetone (8:3) as eluent to afford a dark green solid (46 mg, 52%). ^{1}H-NMR (200 MHz, CD_2Cl_2): 17.5 (s, 1H), 7.49 (d, 1H), 7.48 (s, 1H), 7.26−7.18 (m, 2H), 7.14 (s, 1H), 7.04 (s, 1H), 6.89 (d, 1H), 5.96 (s, 1H), 4.19−3.76 (m, 5H), 2.70 (s, 3H), 2.55 (s, 3H), 2.50 (s, 3H), 2.38 (s, 3H), 2.17 (s, 3H), 1.32 (d, 3H), 1.28 (s, 3H), 1.04 (d, 3H). FAB−MS: m/z $[M - Cl]^+$ Calcd 655.1, found 655.0. Single crystals were successfully grown by slow diffusion of pentane in a solution of **3-Se-*cis*** in CH_2Cl_2 at −18 °C.

$C_{31}H_{38}Cl_2N_2RuSe\cdot CH_2Cl_2$, M = 774.49, monoclinic, space group $C2/c$, a = 20.9440(12), b = 15.2749(7), c = 26.2918(14) Å, β = 95.5333(18)°, V = 8372.0(8) Å^3, Z = 8, T = 110(2) K, ρ_{calcd} = 1.229 gcm^{-3}, μ(Mo Kα) = 1.52 mm^{-1}, 31214 reflections measured ($2\theta_{max}$ = 51.2°), 7621 unique (R_{int} = 0.052), final R = 0.065 (wR = 0.171) for 5817 reflections with $I > 2\sigma(I)$ and R = 0.081 (wR = 0.178) for all data, $\Delta|\rho_{max}|$ = 0.89 e/Å^3. The asymmetric unit of this structure contains at least two additional molecules of severely disordered dichloromethane solvent, which could not be modeled reliably by discrete atoms and were excluded from the final crystallographic refinement.

Diphenyl(2-vinylphenyl)phosphine (22). Methyl triphenylphosphonium iodide (1.56 g, 3.85 mmol) was dissolved in 30 mL of ether in a 100-mL round-bottom flask at 0 °C under dry nitrogen. To the mixture was added in one portion potassium *tert*-butoxide (0.48 g, 4.26 mmol) and the mixture was stirred for 10 min. **21** (0.48 g, 1.65 mmol) was added in one portion at 0 °C and the reaction mixture was stirred for additional 4 h at room temperature. The mixture was added to 150 mL of saturated sodium bicarbonate solution, and extracted with 3 × 50 mL portions of ether. The extracts were dried with magnesium sulfate and evaporated. The light yellow oil of the crude product was further purified by chromatography on silica gel using petroleum ether/CH_2Cl_2 (95:5) as eluent to afford a white solid (326 mg, 69%). ^{1}H-NMR (200 MHz, $CDCl_3$): 7.62−7.55 (m, 1H), 7.41−7.11 (m, 12H), 6.84−6.77 (m, 1H), 5.61 (dt, 1H), 5.20 (dd, 1H). ^{13}C-NMR (50 MHz, $CDCl_3$): 142.6, 142.1, 136.4, 136.2, 135.6, 135.2, 134.1, 133.8, 133.2, 128.9, 128.7, 128.6, 128.4, 127.8, 125.5, 125.4, 116.0. EI−MS: m/z M^+ Calcd 288.11, found 288.15.

Complex 23. (NHC)(Py)$_2$(Cl)$_2$Ru=CHPh (101 mg, 0.14 mmol) and **22** (44 mg, 0.15 mmol) were added to a pressured flask. CH_2Cl_2 (6 mL) was added, the flask was closed, and the mixture was stirred at 40 °C for 5 h. The solvent was evaporated and the product was purified by two recrystallizations from CH_2Cl_2/pentane. A brown solid was obtained after drying (10 mg, 9%). ^{1}H-NMR (500 MHz, CD_2Cl_2): 17.0 (s, 1H), 7.84−7.16 (m, 11H), 7.05 (br s, 4H), 6.78−6.71 (m, 3H), 4.44−3.94 (m, 4H), 2.75 (s, 3H), 2.69 (s, 3H), 2.46 (s, 3H), 2.40 (s, 3H), 2.35 (s, 3H), 2.21 (s, 3H). ESI−MS: m/z $[M - Cl]^+$ Calcd 717.17, found 717.08. Single crystals were successfully grown by slow diffusion of pentane in a solution of **23** in CH_2Cl_2 at −18 °C.

$C_{40}H_{41}Cl_2N_2PRu\cdot CH_2Cl_2$, M = 837.61, monoclinic, space group $P2_1/c$, a = 24.2412(12), b = 15.1628(9), c = 25.3001(11) Å, β = 111.8823(16)°, V = 8629.4(8) Å^3, Z = 8, T = 110(2) K, ρ_{calcd} = 1.289 gcm^{-3}, μ(Mo Kα) = 0.68 mm^{-1}, 52407 reflections measured ($2\theta_{max}$ = 51.0°), 15798 unique (R_{int} = 0.040), final R = 0.068 (wR = 0.174) for 12034 reflections with $I > 2\sigma(I)$ and R = 0.088 (wR = 0.184) for all data, $\Delta|\rho_{max}|$ = 1.47 e/Å^3. The asymmetric unit consists of two crystallographically independent molecules of the organometallic complex. It also contains two additional molecules of a severely disordered dichloromethane solvent, which could not be modeled reliably by discrete atoms and were excluded from the final crystallographic refinement.

Acknowledgment. We thank the Minerva-Stiftung for a short-term grant awarded to C.E.D. to realize part of this research in Heidelberg. The Edmond J. Safra Foundation is gratefully acknowledged for financial support.

Supporting Information Available: NMR and mass spectra analyses, CIF files, and tables of calculated energies and structures. This material is available free of charge via the Internet at http://pubs.acs.org.

(34) Iwaoka, M.; Komatsu, H.; Katsuda, T.; Tomoda, S. *J. Am. Chem. Soc.* **2004**, *126*, 5309–5317.